Carbohydrate Polymers 140 (2016) 35–42

Contents lists available at ScienceDirect

Carbohydrate Polymers

journal homepage: www.elsevier.com/locate/carbpol

Reversible redox activity of ferrocene functionalized hydroxypropyl cellulose and its application to detect H_2O_2

Pingping Li[a,b], Hongliang Kang[a], Chao Zhang[a,b], Weiwei Li[a,b], Yong Huang[a,c,*], Ruigang Liu[a,**]

[a] State Key Laboratory of Polymer Physics and Chemistry, Beijing National Laboratory for Molecular Sciences (BNLMS), Institute of Chemistry, Chinese Academy of Sciences, Beijing 100190, China
[b] University of Chinese Academy of Sciences, Beijing 100049, China
[c] National Research Center for Engineering Plastics, Technical Institute of Physics and Chemistry, Chinese Academy of Sciences, Beijing 100190, China

ARTICLE INFO

Article history:
Received 2 September 2015
Received in revised form
19 November 2015
Accepted 30 November 2015
Available online 10 December 2015

Keywords:
Hydroxypropyl cellulose
Ferrocene
Redox activity
Biosensor
Horseradish peroxidase

ABSTRACT

Novel ferrocene functionalized hydroxypropyl cellulose (HPC-Fc) were prepared by azide-alkyne cycloaddition and characterized. HPC-Fc exhibits an excellent reversible redox activity and could establish amazing electron transfer ability between enzyme and electrode. HPC-Fc and horseradish peroxidase (HRP) were coated on a platinized carbon electrode to prepare an amperometric biosensor for hydrogen peroxide (H_2O_2) detection. The amperometric response was measured as a function of H_2O_2 concentration at a fixed potential of 0.35 V in 100 mM phosphate buffer solution (pH 7.0). The novel biosensor exhibits a fast linear response toward H_2O_2 in the range of 0.1–8 μM with sensitivity of 4.21 nA/μM. Moreover, the enzyme assays measured by the spectrophotometer method confirm that abundant hydroxyl groups of HPC backbones are conductive for HRP to maintaining or even enhancing their activity. The redox active HPC-Fc with the unique properties of both ferrocene and cellulose is a good candidate for biosensor applications.

© 2015 Elsevier Ltd. All rights reserved.

1. Introduction

Cellulose is the most abundant polysaccharides in nature and have been used for thousands years mainly in paper and textile areas (Klemm, Heublein, Fink, & Bohn, 2005). With the increasing demand for eco-friendly and biocompatible materials, cellulosic functional materials with fascinating structures and properties have attracted increasing attentions (Kang, Liu, & Huang, 2013). The hydroxyl groups on cellulose chains offer versatile approaches for the modification of cellulose by either derivation or graft copolymerization to fabricate cellulose functional materials for many purposes, such as tuning the hydrophilic/hydrophobic properties of cellulose (Wang et al., 2011), introducing reactive entities for post-modification strategies (Li et al., 2013), or attaching specific functional groups to permanently modify other cellulose properties (Kang et al., 2012). Typical chemical reactions such as esterification, etherification or silyation reactions have been widely investigated (Klemm et al., 2005; Tingaut, Hauert, & Zimmermann, 2011).

Click reaction is attractive for the synthesis of functional materials due to its unique features of mild reaction conditions, high efficiency, chemoselectivity, simplicity and extraordinary reliability (Espeel & Du Prez, 2015). Cellulosic functional materials with various functional units including oligosaccharides (Negishi, Mashiko, Yamashita, Otsuka, & Hasegawa, 2011), reduced graphene oxide (Kabiri & Namazi, 2014), and α/β-cyclodextrins (Ritter, Knudsen, Mondrzik, Branscheid, & Kolb, 2012), etc. have been synthesized via click reactions. These new cellulosic functional materials have been widely used in the fields of photoactive materials (Huang et al., 2013), antioxidant agents (Trombino et al., 2008) and memory devices (Karakawa et al., 2007) etc. However, the applications of cellulose derivatives in the development of enzyme-based biosensors are still limited (Kang et al., 2012).

Redox-active moieties such as quinone derivatives (Ong, Yang, Cruciano, & McCarley, 2008), ferrocene and its derivatives (Senel, Cevik, & Abasiyanik, 2010), and osmium complex (Kang et al., 2012) are generally used in biosensors to establish efficient electron transfer between electrodes and the target solution species for the detection of H_2O_2 (Senel et al., 2010), glucose (Kang et al., 2012)

* Corresponding author at: State Key Laboratory of Polymer Physics and Chemistry, Beijing National Laboratory for Molecular Sciences (BNLMS), Institute of Chemistry, Chinese Academy of Sciences, Beijing 100190, China. Tel.: +86 10 82618573; fax: +86 10 62559373.
** Corresponding author. Tel.: +86 10 82618573; fax: +86 10 62559373.
E-mail addresses: yhuang@iccas.ac.cn (Y. Huang), rgliu@iccas.ac.cn (R. Liu).

http://dx.doi.org/10.1016/j.carbpol.2015.11.077
0144-8617/© 2015 Elsevier Ltd. All rights reserved.

etc. Among these redox-active moieties, ferrocene has been widely studied in bioelectrochemical systems due to its fast electron transfer, low oxidation potential, and two stable redox states (Eyley et al., 2012; Senel et al., 2010). The development of a redox-active polymer as the mediator in biosensors is essential since leaking of the mediator is suppressed and current densities and analyte sensitivities are higher than that of small redox molecules (Sirkar & Pishko, 1998). Moreover, the properties of the modified electrodes are analyzed by the coverage (concentration) of redox active centers, charge transport and propagation, as well as diffusion and permeation of soluble species through the decorated polymer layer which is greatly affected by the structures of the redox-active polymers (Patrick, Linford, & Hooper, 1987). Specially, the hydrophilicity of redox active polymers is helpful to contact with water-soluble enzymes and preserve their native catalytic structure (Garcia, Peniche-Covas, Chico, Simpson, & Villalonga, 2007; Yang, Zhou, & Sun, 2007), which is one of the most important parameters to achieve analytical devices with higher and faster responses when coupled with oxidoreductase (Dursun et al., 2012; Kang et al., 2012). Cellulose and its hydrophilic derivatives are such promising matrix for the preparation of biosensors (Kang et al., 2012).

In this paper, a series of redox-active cellulose derivatives, ferrocene functionalized HPC (HPC-Fc) were firstly synthesized by click chemistry and characterized. The electrochemical properties of HPC-Fc were investigated via cyclic voltammetry. Furthermore, an amperometric biosensor for the detection of H_2O_2 was fabricated by co-immobilizing of HRP and HPC-Fc on the electrode. The performance of the proposed biosensor towards the quantification of H_2O_2 was also investigated. The cellulose-based redox polymers with the unique redox activity of ferrocene and the hydrophilicity of biocompatible cellulose have the promising applications in the designation of bioelectrochemical devices.

2. Experimental

2.1. Materials

Hydroxypropyl cellulose (HPC, Sigma-Aldrich) was dried 48 h under vacuum at 50 °C before use. The molar degree of substitution of hydroxypropyl groups (the number of hydroxypropyl groups per glucose ring) is 3.56. The molecular weight and its distribution of HPC measured by GPC using THF as the eluent are M_w = 45 100 g/mol and M_w/M_n = 2.15, respectively. 2-Bromoisobutyryl bromide (98%, Sigma-Aldrich), sodium azide (NaN_3, 99.5%, Tianyu Chemical Co. Lt., Zhejiang, China), *N*,*N*′,*N*′,*N*″,*N*‴-pentamethyldiethylenetriamine (PMDETA, Sigma-Aldirch, 98%), ethynylferrocene (J&K, 97%), H_2O_2 (Sigma-Aldrich, 30 wt% in water), horseradish peroxidase (HRP, >200 U/mg, Aladdin), and pyrogallol (≥98%, Sigma-Aldrich) were used as received. CuBr (Sigma-Aldrich, 98%) was stirred in glacial acetic acid at room temperature to remove Cu^{2+}, followed by washing with acetone, and then dried under vacuum at room temperature overnight. Tetrahydrofuran (THF), CH_2Cl_2, $CHCl_3$, pyridine, *N*,*N*-dimethylformamide (DMF), diethyl ether were supplied by Beijing Chemical Works and purified by standard methods before use. The inorganic salts (A.R. grade) were supplied by Sinopharm Chemical Reagent Beijing Co., Ltd and used as received. The water was Milli-Q water.

2.2. Synthesis of ferrocene-functionalized hydropropyl cellulose (HPC-Fc)

The synthesis route of HPC-Fc is shown in Scheme 1. Bromoisobutyl hydropropyl cellulose (HPC-Br) was firstly synthesized according to previous works (Ma et al., 2010; Xu et al., 2009). The synthetic process of HPC-Br is described in details in ESI.

The preparation of azide functionalized hydropropyl cellulose (HPC-N_3) was performed through azidation of HPC-Br according to literatures (Eyley et al., 2012). Briefly, HPC-Br (DS_{Br} = 0.26, 1.0 g, 0.54 mmol Br) was dissolved in 100 mL DMF and then NaN_3 (39 mg, 0.59 mmol) was added. The reaction mixture was stirred at 30 °C for 48 h and then dialyzed against deionized water for one week to remove solvent and unreacted NaN_3. The resulted solution was lyophilized to obtain HPC-N_3 (1.01 g, yield: 97%). The degree of substitution of aizde groups can be controlled by the amount of NaN_3 added in the reaction mixture and DS_{Br} of HPC-Br. In this work, excess NaN_3 was used to ensure the complete substitution of bromide atoms with azide groups.

The synthesis of HPC-Fc was performed typically as follows (Eyley et al., 2012; Ritter et al., 2012). HPC-N_3 (DS_{N3} = 0.25, 0.5 g, 0.31 mmol) and ethynylferrocene (72 mg, 0.34 mmol) were dissolved in a Schlenk flask with 50 mL degassed DMF. Then 11 mg (0.08 mmol) of CuBr and 20 μL (0.096 mmol) of PMDETA were added. The flask was sealed, and the reaction mixture was degassed by three cycles of freezing-pumping-thawing. Then the flask was immersed into an oil bath keeping at 80 °C to carry out the reaction for 24 h. The reaction mixture was diluted with THF and then passed through a basic alumina column to remove the copper complex. The solution was concentrated and then precipitated in excess diethyl ether to obtain HPC-Fc (0.49 g, yield: 96.7%) after drying in vacuum at 40 °C.

2.3. Modification of electrode

Prior to the modification of the platinized carbon working electrode, the bare electrode (Φ 3 mm) was firstly polished with alumina powder (0.1 and 0.05 μm, respectively) on chamois leather, followed by sonication, rinse with water and then ethanol. For modification of the electrode, 5 μL of HPC-Fc solution (2 mg/mL in $CHCl_3$) was dropped on the glassy carbon electrode and then dried at room temperature for 6 h. For the preparation of biosensor with HPC-Fc and HRP enzyme, 5 μL of HPC-Fc in $CHCl_3$ (2 mg/mL) was dropped onto the glassy carbon electrode and dried in air. And then 5 μL of HRP solution (5 mg/mL in 100 mM, pH 7.0 PBS) was further dropped onto the electrode coated by HPC-Fc and left in air for 4 h to dry. The modified electrode was washed with PBS and stored at 4 °C.

2.4. Characterization

^{1}H NMR measurements were carried out on a Bruker Advance 400 MHz NMR spectrometer in $CDCl_3$ solution with tetramethylsilane as an internal standard. FTIR spectra were recorded on a Bruker-Equinox 55 FT-TR spectrometer with the resolution of 4 cm^{-1} by KBr pallet technique. The molecular weight and its distribution of polymers were measured on gel permeation chromatography (GPC, Waters 410). Mono-dispersed polystyrene was used as the standard and THF was used as the eluent at the flow rate of 1 mL/min. The content of Fe in HPC-Fc was determined by inductively coupled plasma atomic emission spectroscopy (ICP-AES, Varian 710-ES, U.S.).

UV–vis spectra were recorded on a UV–vis spectrophotometer (Shimadzu, UV-1901). The concentration of HPC-Fc was kept at 5 mg/mL in $CHCl_3$.

Electrochemical properties were carried out on a CHI660D electrochemical workstation (Chenhua Inst. Corp., Shanghai, China). A conventional three-electrode system composed of a platinized carbon electrode as working electrode, a Pt wire as counter electrode and Ag/AgCl-saturated KCl as the reference electrode was used in the electrochemical measurements. The supporting

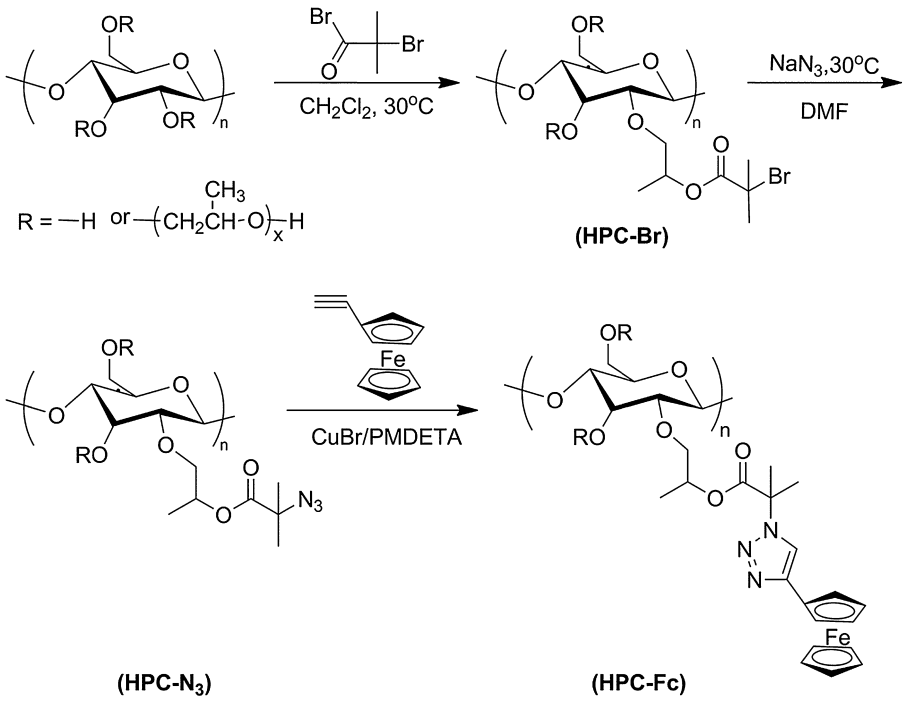

Scheme 1. Synthetic route of HPC-Fc.

electrolyte, 100 mM, pH 7.0 phosphate buffer solution (PBS) was maintained under argon atmosphere during each measurement. Cyclic voltammetry (CV) experiments were carried out at ambient temperature with certain scan rate in the potential range of 0–0.6 V. Amperometric measurements were carried out at room temperature in stirred solution by applying the desired potential and allowing the steady-state current to be reached. Once prepared, the HPC-Fc/HRP electrode was immersed in 20 mL PBS and the amperometric responses to hydrogen peroxide were recorded upon successive addition of certain amount of hydrogen peroxide solution into the PBS. Three measurements were carried out, by which the average value and error bar for each data point were estimated. Electrochemical impedance spectroscopy (EIS) experiments were performed at an open circuit potential of 500 mV within the frequency range of 10^{-1}–10^{5} Hz in 0.1 M KCl solution containing 5.0 mM $K_3Fe(CN)_6/K_4Fe(CN)_6$ (molar ration 1:1) as the redox probe.

Enzyme assays were performed on a UV–vis spectrophotometer (Shimadzu, UV-1901) to determine the activity of HRP after mixing with HPC or HPC-Fc by spectrophotometric method (Sirkar & Pishko, 1998). The absorbance at 420 nm were used to determine the concentration of the substrate (H_2O_2) catalyzed by HRP. The specific operations are as follows: Pyrogallol and HRP (HPC/HRP or HPC-Fc/HRP) in PBS were firstly mixed in a quartz cuvette, and then the substrate was added into the mixture. The production of the colored assay product was monitored as a function of time at 420 nm and activity was determined from the linear slope of the absorbance-time plot. Three measurements were carried out, by which the average data and errors were estimated.

3. Results and discussion

3.1. Synthesis of HPC-Fc

The synthesis route of HPC-Fc is shown in Scheme 1. ^{1}H NMR (Fig. 1a) and FTIR (Fig. 1b) spectra confirm the successful synthesis of HPC-Br, and the details have been discussed in previous works (Ma et al., 2010). The degree of substitution of bromide groups (DS_{Br}, numbers of bromine atoms per glucose ring) can be estimated by comparing the integral areas of the proton signal at around δ = 1.1 ppm for the methyl group in HPC to that of methyl group in the 2-bromoisobutyl groups of HPC-Br at around δ = 1.92 ppm (Fig. 1a, a′), which can be controlled by adjusting the feeding mole ratio of 2-bromoisobutyl bromide to HPC. The reaction conditions and DS_{Br} of the resultant HPC-Br are listed in Table 1.

HPC-N_3 was obtained by the azidation of HPC-Br performed with azide sodium. Both ^{1}H NMR (Fig. 1a) and FTIR (Fig. 1b) spectra confirm that bromine atoms of HPC-Br are completely replaced by azide groups. On the ^{1}H NMR spectrum of HPC-N_3 (Fig. 1a), the characteristic proton peaks of methyl groups in 2-azidoisobutyl groups shift from δ = 1.92 ppm to δ = 1.46 ppm (Fig. 1a, a″). The degree of substitution of azide groups (DS_{N3}) can be calculated by comparing the integral area of the methyl proton of HPC at around δ = 1.1 ppm to that of the peak at δ = 1.46 ppm attributed to the methyl proton of 2-azidoisobutyl groups. The value is almost similar to that of DS_{Br}. On the FTIR spectra of HPC-N_3 (Fig. 1b), the characteristic band at 2111 cm^{-1} is attributed to the stretching vibration of the —N=N=N groups which confirms the substitution of bromide atoms with azide groups. DS_{N3} of the obtained HPC-N_3 depends on DS_{Br} of the starting HPC-Br and the amount of azide sodium added to perform the azidation of HPC-Br. The reaction conditions and DS_{N3} of the corresponding HPC-N_3 are listed in Table 1.

The alkyne-azide click chemistry of HPC-N_3 was successfully carried out with ethynylferrocene catalyzed by CuBr/PMDETA in DMF to yield HPC-Fc. The ethynylferrocene was added in a slight excess to ensure the complete reaction of azide groups in HPC-N_3 by the click reaction. The chemical structure of HPC-Fc was characterized by ^{1}H NMR (Fig. 1a) and FTIR spectra (Fig. 1b). The characteristic resonances peaks at δ = 4.06, 4.29 and 4.73 ppm are attributed to the nine protons of ferrocenyl, which are marked clearly on the ^{1}H NMR spectrum of HPC-Fc (Fig. 1a). The peak at δ = 1.46 ppm attributed to the methyl proton of 2-azidoisobutyl groups disappears and a new characteristic peak of the corresponding methyl proton appears at δ = 1.96 ppm compared with the ^{1}H NMR spectrum of HPC-N_3 (Fig. 1a). After the click chemistry, the characteristic band of azide groups at 2111 cm^{-1} on the FTIR spectrum of HPC-N_3 disappeared with the appearance of the

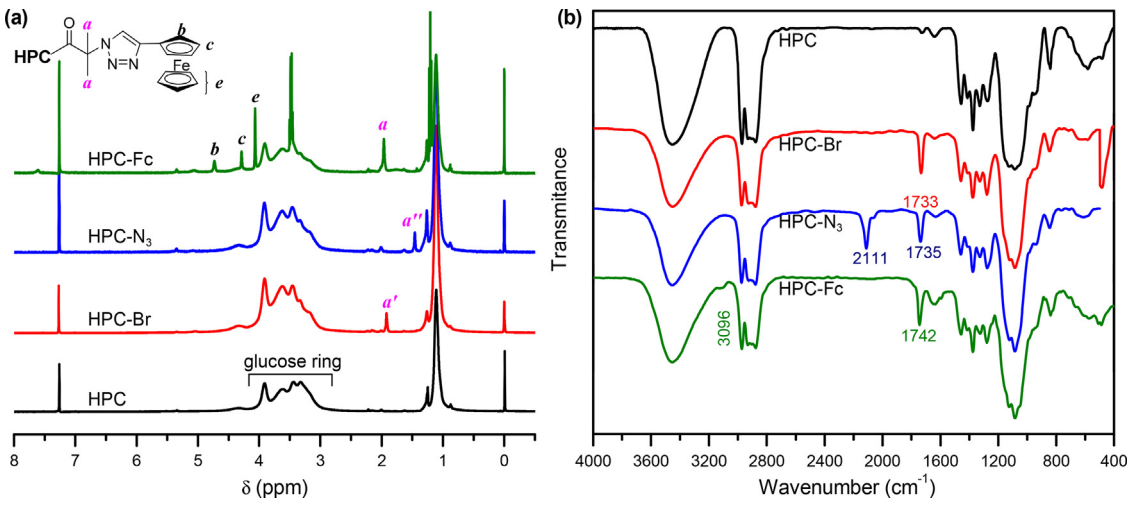

Fig. 1. ^{1}H NMR (a) and FTIR (b) spectra of HPC, HPC-Br, HPC-N_3, and HPC-Fc.

characteristic band of ferrocene rings at 3096 cm^{-1} on the FTIR spectrum of HPC-Fc. HPC-Fc was further characterized by UV–vis absorption spectra (see ESI, Fig. S1). Compared to the UV–vis spectra of HPC-Br and HPC-N_3, a peak at 445 nm corresponding to the characteristic peak of the neutral ferrocene state appears on the spectrum of HPC-Fc (see ESI, Fig. S1). The content of Fe in HPC-Fc was determined by ICP-AES, which depend on the DS_{N3} of HPC-N_3 and the amount of ethynylferrocene added to perform the click reaction. The molecular weight and distribution of HPC-Fc were estimated by GPC. The results show that the molecular weight of HPC-Fc increases with the content of Fe and its distribution can be comparable with that of HPC. The ICP-AES and GPC results are shown in Table 1.

The degree of substitution of the ferrocenyl groups (DS_{Fc}) was estimated by ^{1}H NMR spectra by

$$DS_{Fc} = \frac{\sum A_{Fc}}{A_{HPC\text{-}methyl}} \times \frac{MS_{HP} \times 3}{9} \quad (1)$$

where $\sum A_{Fc}$ is the sum of the integral areas corresponding to the nine protons of ferrocenyl groups at δ = 4.06, 4.29, and 4.73 ppm and $A_{HPC\text{-}methyl}$ is the integral areas of the methyl protons of HPC at δ = 1.1 ppm as indicated on the ^{1}H NMR spectrum of HPC-Fc (Fig. 1a). MS_{HP}, the molar degree of substitution of hydroxypropyl groups per glucose ring on HPC backbone, is 3.56. DS_{Fc} of HPC-Fc is determined by DS_{Br} of HPC-Br and DS_{N3} of HPC-N_3. DS_{Fc} can also be estimated by the results of ICP-AES and UV–vis spectra analysis (Yang et al., 2007). DS_{Fc} of HPC-Fc has the similar values through three different measurement methods. The details of the synthesis conditions and the resulted HPC-Fc are listed in Table 1.

3.2. Redox activity (electrochemical property) of HPC-Fc

The electrochemical properties of the redox HPC-Fc were firstly studied through cyclic voltammetry in a PBS after casted onto a glassy carbon electrode. Fig. 2a shows the CVs of HPC-$Fc_{0.25}$ at different potential scan rates. A pair of symmetrical redox peaks corresponding to the oxidation potential (E_{pa}) and reduction potential (E_{pc}) are observed (Fig. 2a). Obviously, this is a one-electron redox reaction of HPC-Fc^+/HPC-Fc, indicating that all electroactive ferrocenyl moieties of HPC-Fc possess the same redox potential. The E_{pa} and E_{pc} at the potential scan rate of 100 mV/s are 0.381 V and 0.336 V, respectively. With the potential scan rates increasing, the CV peak currents of the HPC-Fc modified electrode increased in the scan rates of 10–500 mV/s accompanied by the slightly increase of the peak to peak separation ($\Delta E_p = E_{pa} - E_{pc}$). However, all the ΔE_p at the potential scan rates of ≤500 mV/s are no more than $59/n$ mV (n = 1, the number of electrons acts characteristic of the ferrocene electrochemistry), indicating that the HPC-Fc was efficiently connected to the GCE for fast and reversible electron transfer. The CV peak currents (I_p) increase linearly with the square root of the potential scan rate ($v^{1/2}$) (Fig. 2b). The above results suggest that the electrochemical behavior of HPC-Fc is diffusion controlled quasi-reversible process according with the electron transport model of Randles–Sevcik (Eq. (2)).

Table 1
Synthesis conditions and the corresponding HPC-Fc.[a]

Run	[BiB]:[—OH][b]	DS_{Br}	[—Br]:[NaN_3][c]	DS_{N3}	[—N_3]:[ethybyl][d]	DS_{Fc}[e]			Fe cont. (%)[f]	M_w (g/mol)[g]	M_w/M_n[g]
						^{1}H NMR	UV–vis	ICP			
1	1:35	0.03	1:1.1	0.04	1:1.1	–	0.04	0.04	0.61	47 200	3.2
2	1:24	0.06	1:1.1	0.07	1:1.1	–	0.07	0.08	1.14	48 500	3.0
3	1:11	0.17	1:1.1	0.16	1:1.1	0.17	0.16	0.18	2.36	51 400	2.7
4	1:8	0.19	1:1.1	0.20	1:1.1	0.20	0.21	0.19	2.48	53 000	2.9
5	1:6	0.26	1:1.1	0.25	1:1.1	0.23	0.24	0.25	3.12	55 000	2.4

[a] In the following context, HPC-Fc is presented as HPC-Fc_{xx} and the subscript "*xx*" represents the degree of substitution of ferrocene moieties (DS_{Fc}).
[b] The mole ratio of 2-bromoisobutyryl bromide (BriB) to hydroxyl group of HPC for synthesis of HPC-Br.
[c] The mole ratio of bromoisobutyryl groups of HPC-Br to NaN_3 used to synthesize HPC-N_3.
[d] The mole ratio of azide groups of HPC-N_3 to ethynylferrocene for the click reaction.
[e] DS_{Fc} calculated from the results of ^{1}H NMR, ICP, UV–vis.
[f] Iron content in the HPC-Fc is determined by ICP-AES.
[g] Determined by GPC.

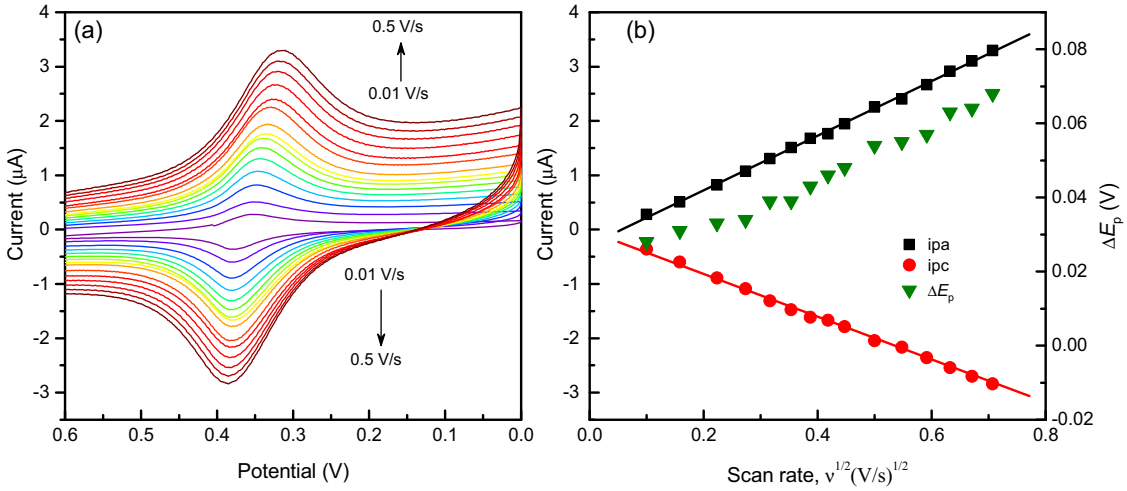

Fig. 2. (a) Cyclic voltammograms of the HPC-$Fc_{0.25}$ modified electrode obtained at different potential scan rates; (b) The peak current and peak-to-peak separation dependence on the square-root of the potential scan rate. The measurements were performed in 100 mM phosphate buffer, pH 7.0.

The diffusion coefficient of charge transfer (D_{ct}) was determined by the following equation (Sirkar & Pishko, 1998),

$$I_p = 0.4463(nF)^{3/2}AC^* \times \left(D_{ct}\nu/RT\right)^{1/2} \quad (2)$$

where I_p is the peak current, n is the number of electrons, F is Faraday's constant, D_{ct} is the diffusion coefficient of charge transfer, C^* is the concentration of ferrocene redox centers in the film, ν is the scan rate, R is the universal gas constant, A is the electrode area in cm^2 and T is temperature. The ${D_{ct}}^{1/2}C^*$ of the HPC-$Fc_{0.25}$ was estimated at the level of 10^{-10} mol/cm^2 $s^{1/2}$, which is similar to other redox polymers (Sirkar & Pishko, 1998). Electron-transfer under diffusion control suggests that three-dimensional charge propagation in the HPC-Fc is through electron-hopping between neighboring ferrocene redox sites in a concentration gradient.

Table 2 lists the half-wave potential [$E^\theta = (E_{pa} + E_{pc})/2$], peak to peak separation ($\Delta E_p = E_{pa} - E_{pc}$), ratios of anodic to cathodic peak currents (I_{pa}/I_{pc}) and ${C^*D_{ct}}^{1/2}$ for HPC-Fc with different substitution degree of ferrocenyls. The electrochemical properties of the HPC-Fc modified electrode are affected by the ferrocenyl functionalization level, i.e., degree of distribution of ferrocenyl groups (DS_{Fc}) (Table 2). As shown in Table 2 and Fig. S2 (in ESI), both the oxidation and the reduction peaks shift anodically, whereas a slight positive shift of the formal potential (E^θ) is observed for HPC-Fc with higher DS_{Fc}, which may be due to the different environments of the redox–active groups ferrocenyl on the electrodes. In addition, the slope of the linear correlation between I_p and $\nu^{1/2}$ is found to be increasing with the increase of concentration of ferrocene redox centers in the film, which suggests that ${C^*D_{ct}}^{1/2}$ calculated by the Randles–Sevcik equation is also affected by DS_{FC}. The parameters given in Table 2 show that the HPC-Fc modified electrode possess quasi-reversible electrochemical characteristics.

3.3. Application for H_2O_2 detection

HPC-Fc was further used as a matrix for the non-covalent immobilization of HRP on a bare platinized carbon working electrode to prepare an amperometric biosensor for hydrogen peroxide (H_2O_2) detection. The preparation process of enzyme electrodes was monitored by CV and EIS (see ESI, Figs. S3 and S4, respectively). Compared with CV curves of the bare GCE and HPC modified electrode with no peaks (see ESI, Fig. S3), typical symmetrical redox-response peaks of ferrocenyl groups are observed on the CV curves of HPC-Fc and HPC-Fc/HRP electrodes. However, peak current of the HPC-Fc/HRP enzyme electrode are obviously smaller than that of HPC-Fc electrode, which may be due to the hindrance of HRP to the electron transfer.

The interface properties of the modified electrodes were further investigated by EIS. (Liang, Fan, Wang, & Qiu, 2009) Fig. S4 shows the EIS results of bare GCE, HPC/GCE, HPC-Fc/GCE and HPC-Fc/HRP/GCE in the presence of redox probe $Fe(CN)_6^{3-/4-}$ (see ESI). It can be seen that the Nyquist plot (Z'' versus Z') of bare GCE is an almost straight line, indicating a diffusion limited process. However, clear semicircle portions can be observed on Nyquist plots of the modified electrodes. Semicircle diameter is in the order of HPC/GCE > HPC-Fc/HRP/GCE > HPC-Fc/GCE, indicating the decrease in electron transfer resistance. The electron transfer resistance of the HPC-Fc modified electrode obviously decreased by comparison with that of the HPC modified electrode, which is due to the improvement in the conductivity by the coating of HPC-Fc. An increase in the electron transfer resistance was observed after the immobilization of HRP on the electrode, indicating that HRP acts as a barrier for the electron transfer. The changes of EIS during the modified process of the electrode indicate that HPC-Fc and HRP are successfully coated on electrodes and the smaller electron transfer resistance contributes to electrochemical detection. These results are consistent with the CV results.

Fig. 3A is CV curves of HPC/HRP, and HPC-Fc/HRP enzyme electrode in 100 mM, pH 7.0 PBS in the absence and presence of H_2O_2 at the scan rate of 100 mV/s. As shown in Fig. 3A-a, HPC-Fc/HRP enzyme electrode shows the typical redox-response peaks of the redox-active ferrocenyl groups in the absence of H_2O_2. When H_2O_2 is added into the solution, an obvious increase in the reduction current was observed, accompanied by a dramatic decrease in the anodic peak current (Fig. 3A-b). The electrocatalytic behavior of HPC-Fc/HRP enzyme electrode in the reduction of hydrogen peroxide is similar to that in literature (Garcia et al., 2007). This result proves that the electron-transfer between the enzyme and electrodes is mediated by the ferrocene redox centers on the HPC backbone. The reaction mechanism of the typical enzyme-dependent electrocatalytic processes for the determination of H_2O_2 can be explained by the following equations (Eqs. (3)–(6)) (Eyley et al., 2012),

$$H_2O_2 + HRP \rightarrow H_2O + HRP(I) \quad (3)$$

$$HRP(I) + HPC\text{-}Fc \rightarrow HRP(II) + HPC\text{-}Fc^+ \quad (4)$$

$$HRP(II) + HPC\text{-}Fc \rightarrow HRP + HPC\text{-}Fc^+ \quad (5)$$

$$HPC\text{-}Fc^+ + 2e^- \rightarrow HPC\text{-}Fc \quad (6)$$

Table 2
Electrochemical properties of HPC-Fc with different DS of ferrocenyl groups.

Samples	Oxidation peak E_{pa} (V)[a]	Reduction peak E_{pc} (V)[a]	ΔE_p (V) = $E_{pa} - E_{pc}$[a]	I_{pa}/I_{pc}[a]	E^{θ}(V) = ($E_{pa} + E_{pc}$)/2[a]	$C^{*}D_{ct}^{1/2} \times 10^{10}$ (mol/cm^2 s$^{1/2}$)[b]
HPC-$Fc_{0.04}$	0.338	0.272	0.066	0.97	0.305	–
HPC-$Fc_{0.07}$	0.343	0.281	0.062	1.11	0.312	1.27
HPC-$Fc_{0.16}$	0.369	0.324	0.045	1.27	0.347	4.09
HPC-$Fc_{0.20}$	0.385	0.330	0.055	1.19	0.358	5.96
HPC-$Fc_{0.25}$	0.381	0.336	0.045	1.35	0.359	4.17

[a] All the results of cyclic voltammograms listed in the table are performed at a scan rate of 100 mV/s.
[b] Calculated from the respective Randles–Sevcik equation.

H_2O_2 is firstly reduced to water while HRP is oxidized to HRP (I) (Eq. (3)). In the following, HRP is recovered by the HPC-Fc mediator through two separate steps (Eqs. (4) and (5)), which means that HRP(I) is first oxidized to HRP(II) and then HRP(II) is reduced back to HRP, with the mediator HPC-Fc oxidized to HPC-Fc^+. Finally, HPC-Fc^+ is reduced to HPC-Fc in the neutral state at the electrode as the mediator, producing an increase of its reduction current (Eq. (6)).

Based on the excellent bioelectrocatalytic response to the reduction of H_2O_2, the HPC-Fc/HRP enzyme electrode can be used as an amperometric biosensor to detect H_2O_2. The amperometric response of the modified electrode to successive addition of H_2O_2 was evaluated by applying a fixed potential of +0.35 V because of higher electroanalytic response and a lower noise/signal ratio at this working potential. Fig. 3B illustrates a typical current-time plot for the HPC-Fc/HRP enzyme electrode on stepwise addition of H_2O_2. The results indicate that the biosensor is sensitive to the concentration of H_2O_2 and the reduction current obviously increases with the concentration of H_2O_2 rising, which follows the Michaelis–Menten kinetics (Garcia et al., 2007). The calibration curve of the response current of the enzyme electrode versus H_2O_2 concentration is shown in Fig. 3C. A well-defined linear relation of reduction currents and the concentration of H_2O_2 has been observed in the range from 0.1 to 8 μM and then a plateau is reached gradually at higher H_2O_2 concentration. The HPC-Fc/HRP electrode has a good detection limit of 0.1 μM with a short response time and a high sensitivity of 4.21 nA/μM which is calculated from the linear region of the calibration curve. And the Michaelis–Menten constant (K_M) calculated by analyzing the slope and intercept for the plot of the reciprocals of the anodic current vs. H_2O_2 concentration is 1.05 mM in this work, and the details are shown in ESI.

The stability and reproducibility of the HPC-Fc/HRP enzyme electrode can be estimated by measuring the amperometric response to a certain amount of H_2O_2. The enzyme electrodes show acceptable stability and reproducibility for the detection of H_2O_2. It was found that the amperometric response to H_2O_2 decreased only 10% after the enzyme electrode was tested for the first 18 times continuously, and 70% of the initial response was maintained with subsequent use (see ESI, Fig. S5a). For estimation of the stability, the enzyme electrode was stored at 4 °C in a refrigerator and the properties of the electrode were checked from time to time. The results indicate that the enzyme electrode is quite stable during the storage. About 90% of the responsive properties remained 2 weeks storage (see ESI, Fig. S5b). The reproducibility of one single enzyme electrode was evaluated with the variation coefficients of <2% and 2.3% for 5 successive assays at H_2O_2 concentration of 5 μM and 7 μM, respectively. What's more, three electrodes were fabricated independently under the same condition and used for amperometric measurement at the H_2O_2 concentration of 5 μM. The enzyme electrodes show a relative standard deviation of ~4.8% for the response to the same concentration of H_2O_2, displaying an acceptable reproducibility.

Compared with previous HRP enzyme electrodes with ferrocene or its derivatives as electron transfer mediators for the bioelectroanalytic determination of H_2O_2, the performance of the biosensor in this work is excellent and the results are listed in Table 3. HPC-Fc/HRP enzyme electrode exhibits high sensitivity, low detection limit, fast response time, small K_M, good stability and reproducibility, suggesting that the enzyme electrode exhibits high affinity to H_2O_2 and the catalytic activity of HRP is retained probably by the non-covalent approach and the hydrophilic microenvironment around the immobilized HRP provided by the HPC backbones.

The above results confirm that HPC-Fc can be effectively employed as an excellent mediator for the fabrication of H_2O_2 biosensors with excellent performance, which can be explained from following two aspects: (1) the electron-transfer process between HRP and the electrode mediated by ferrocene redox sites attached to the HPC backbones for the reduction of H_2O_2 is actually efficient; (2) the HPC backbone with amounts of hydroxyl groups

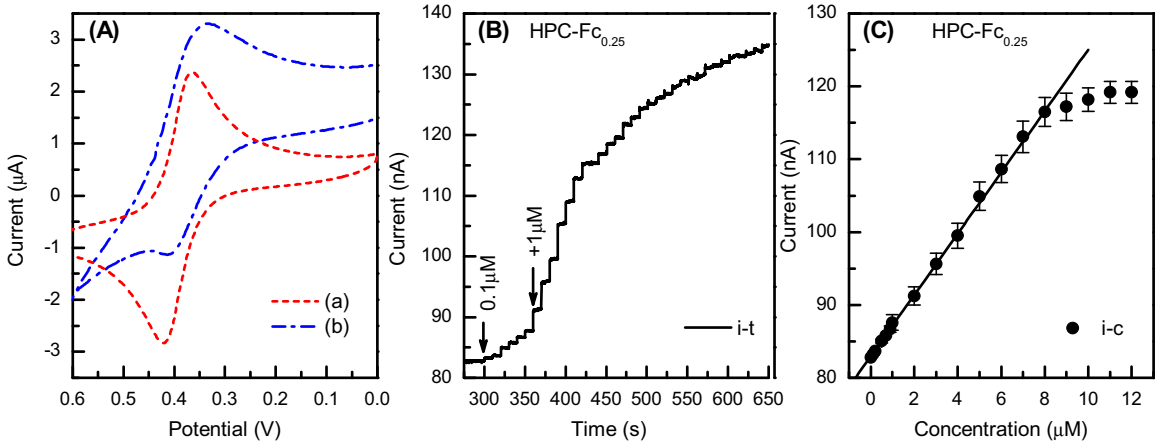

Fig. 3. (A) Cyclic voltammograms of HPC-Fc/HRP electrode at 100 mV/s in 100 mM PBS at pH 7.0, in the absence (a) and presence (b) of H_2O_2. (B) Current-time curve obtained at a HPC-$Fc_{0.25}$/HRP film electrode upon successive addition of H_2O_2 solution to 100 mM PBS (pH 7.0) with an applied potential of 0.35 V. (C) Calibrated curve of the biosensor with successive addition of H_2O_2.

Table 3
Comparison of the performance of the H_2O_2 biosensor based on HRP.

Electrode	RT (s)	Linear range	Detection limit	Sensitivity	Refs.
GCE/P(GMA-*co*-VFc)	4	2.0–30 mM	2.6 μM	0.74 nA/mM	Eyley et al. (2012)
GCE/CHIT-Fc	–	0.035–2 mM	15.0 μM	28.4 μA/mM	Garcia et al. (2007)
GCE/P(m-AAMFc)	–	0.08–15 μM	0.08 μM	34 nA/μM	Mulchandani and Pan (1999)
FMC-BSA/MWNTs/ormosil	5	0.02–4.0 mM	5.0 μM	0.042 μA/mM	Tripathi, Kandimalla, and Ju (2006)
β-CD-Au/HRP-ADA	6	12–450 μM	5.0 μM	1.02 mA/M cm^2	Camacho et al. (2007)
GCE/P(GMA-*co*-VFc)	4	2.0–30 mM	2.6 μM	10.42 nA/mM cm^2	Senel et al. (2010)
Au/HRP-AuNP	15	0.02–13.7 mM	3.0 μM	40.1 mA/M cm^2	Chico et al. (2009)
Au/PolyAuNP/HRP	–	0.005–1.1 mM	2.0 μM	498 μA/M cm^2	Villalonga, Diez, Yanez-Sedeno, and Pingarron (2011)
GCE/HRP/sol-gel/MWNTs	–	0.07–3 mM	14 μM	–	Xu, Li, Zhou, and Zhang (2014)
p-CD-Au/HRP-ADA/HRP	10 s	0.1–3.9 mM	2.0 μM	720 μA/M cm^2	Camacho et al. (2008)
GCE/HPC-Fc	–	0.1–8 μM	0.1 μM	4.21 nA/μM	This work

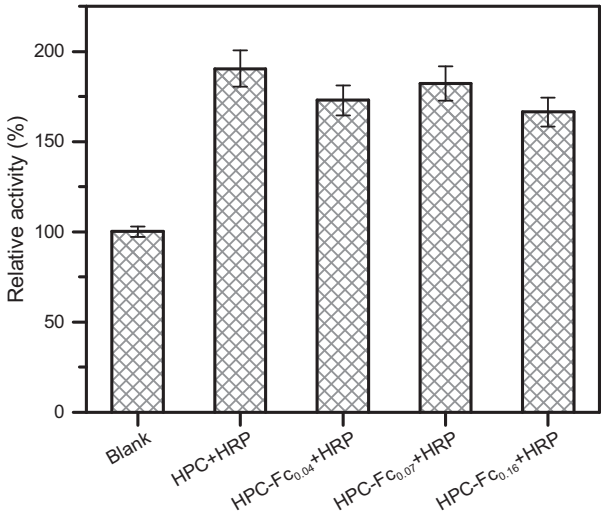

Fig. 4. Comparison of enzyme activity of the HRP, HPC + HRP, HPC-$Fc_{0.04}$ + HRP, HPC-$Fc_{0.07}$ + HRP and HPC-$Fc_{0.16}$ + HRP. The measurements were performed in 100 mM phosphate buffer, pH 7.0.

confers a highly hydrophilic microenvironment to enzyme to preserve their catalytic properties and favor to their re-use (Dursun et al., 2012), which is evidenced by the enzyme activity of the HPC-Fc/HRP composites as shown in Fig. 4. Compared with the blank HRP of 100%, the enzyme activity of HRP is enhanced to about 200% when mixing with HPC as it provides the hydrophilic microenvironment for enzyme entrapment. Despite the result that the enzyme activity slightly decreases to approximately 180% after mixing with the ferrocene modified HPC derivative (HPC-Fc), the activity is still higher than that of pure HRP.

4. Conclusion

Novel ferrocene functionalized hydroxypropyl cellulose (HPC-Fc) was synthesized successfully by azide-alkyne cycloaddition. Results show that HPC-Fc with excellent reversible redox activity can be used as an attractive biopolymer mediator. Co-immobilization of HRP and the redox active polymer (HPC-Fc) on the electrode can be effectively employed for the fabrication of hydrogen peroxide detection sensor. The biosensor exhibits a good linear electroanalytic response toward H_2O_2 in the range of 0.1–8 μM and a high sensitivity for H_2O_2 of about 4.21 nA/μM. Moreover, abundant hydroxyl groups of the HPC backbones with a suitable hydrophilic microenvironment contribute to enzyme activity and their re-use. Therefore, it is believed that the redox polymer based on HPC has promising perspectives for the construction of other enzyme biosensor or bioelectronic devices.

Acknowledgement

The financial support of the National Natural Science Foundation of China (Grant Nos. 2117450, 21274154) is greatly appreciated.

Appendix A. Supplementary data

Supplementary data associated with this article can be found, in the online version, at doi:10.1016/j.carbpol.2015.11.077.

References

Camacho, C., Matias, J. C., Cao, R., Matos, M., Chico, B., Hernandez, J., et al. (2008). Hydrogen peroxide biosensor with a supramolecular layer-by-layer design. *Langmuir*, *24*(15), 7654–7657.
Camacho, C., Matias, J. C., Chico, B., Cao, R., Gomez, L., Simpson, B. K., et al. (2007). Amperometric biosensor for hydrogen peroxide, using supramolecularly immobilized horseradish peroxidase on the β-cyclodextrin-coated gold electrode. *Electroanalysis*, *19*(24), 2538–2542.
Chico, B., Camacho, C., Perez, M., Longo, M. A., Sanroman, M. A., Pingarron, J. M., et al. (2009). Polyelectrostatic immobilization of gold nanoparticles-modified peroxidase on alginate-coated gold electrode for mediatorless biosensor construction. *Journal of Electroanalytical Chemistry*, *629*(1–2), 126–132.
Dursun, F., Ozoner, S. K., Demirci, A., Gorur, M., Yilmaz, F., & Erhan, E. (2012). Vinylferrocene copolymers based biosensors for phenol derivatives. *Journal of Chemical Technology and Biotechnology*, *87*(1), 95–104.
Espeel, P., & Du Prez, F. E. (2015). "Click"-inspired chemistry in macromolecular science: Matching recent progress and user expectations. *Macromolecules*, *48*(1), 2–14.
Eyley, S., Shariki, S., Dale, S. E. C., Bending, S., Marken, F., & Thielemans, W. (2012). Ferrocene-decorated nanocrystalline cellulose with charge carrier mobility. *Langmuir*, *28*(16), 6514–6519.
Garcia, A., Peniche-Covas, C., Chico, B., Simpson, B. K., & Villalonga, R. (2007). Ferrocene branched chitosan for the construction of a reagentless amperometric hydrogen peroxide biosensor. *Macromolecular Bioscience*, *7*(4), 435–439.
Huang, Y. Z., Kang, H. L., Li, G. H., Wang, C. Y., Huang, Y., & Liu, R. G. (2013). Synthesis and photosensitivity of azobenzene functionalized hydroxypropylcellulose. *RSC Advances*, *3*(36), 15909–15916.
Kabiri, R., & Namazi, H. (2014). Surface grafting of reduced graphene oxide using nanocrystalline cellulose via click reaction. *Journal of Nanoparticle Research*, *16*(7), 13.
Kang, H. L., Liu, R. G., & Huang, Y. (2013). Cellulose derivatives and graft copolymers as blocks for functional materials. *Polymer International*, *62*(3), 338–344.
Kang, H. L., Liu, R. G., Sun, H. F., Zhen, J. M., Li, Q. M., & Huang, Y. (2012). Osmium bipyridine-containing redox polymers based on cellulose and their reversible redox activity. *Journal of Physical Chemistry B*, *116*(1), 55–62.
Karakawa, M., Chikamatsu, M., Yoshida, Y., Azumi, R., Yase, K., & Nakamoto, C. (2007). Organic memory device based on carbazole-substituted cellulose. *Macromolecular Rapid Communications*, *28*(14), 1479–1484.
Klemm, D., Heublein, B., Fink, H. P., & Bohn, A. (2005). Cellulose: Fascinating biopolymer and sustainable raw material. *Angewandte Chemie-International Edition*, *44*(22), 3358–3393.
Li, W. W., Liu, R. G., Kang, H. L., Sun, Y. M., Dong, F. Y., & Huang, Y. (2013). Synthesis of amidoxime functionalized cellulose derivatives as a reducing agent and stabilizer for preparing gold nanoparticles. *Polymer Chemistry*, *4*(8), 2556–2563.
Liang, R. P., Fan, L. X., Wang, R., & Qiu, J. D. (2009). One-step electrochemically deposited nanocomposite film of CS-Fc/MWNTs/GOD for glucose biosensor application. *Electroanalysis*, *21*(15), 1685–1691.
Ma, L., Liu, R. G., Tan, J. J., Wang, D. Q., Jin, X., Kang, H. L., et al. (2010). Self-assembly and dual-stimuli sensitivities of hydroxypropylcellulose-*graft*-poly(*N*,*N*-dimethyl aminoethyl methacrylate) copolymers in aqueous solution. *Langmuir*, *26*(11), 8697–8703.

Mulchandani, A., & Pan, S. T. (1999). Ferrocene-conjugated *m*-phenylenediamine conducting polymer-incorporated peroxidase biosensors. *Analytical Biochemistry*, *267*(1), 141–147.
Negishi, K., Mashiko, Y., Yamashita, E., Otsuka, A., & Hasegawa, T. (2011). Cellulose chemistry meets click chemistry: Syntheses and properties of cellulose-based glycoclusters with high structural homogeneity. *Polymers*, *3*(1), 489–508.
Ong, W., Yang, Y. M., Cruciano, A. C., & McCarley, R. L. (2008). Redox-triggered contents release from liposomes. *Journal of the American Chemical Society*, *130*(44), 14739–14744.
Patrick, A. J., Linford, R. G., & Hooper, A. (1987). Structure and composition of composite cathodes used in solid-state lithium polymeric batteries. *Journal of the Electrochemical Society*, *134*(3). C146-C146
Ritter, H., Knudsen, B., Mondrzik, B. E., Branscheid, R., & Kolb, U. (2012). Cellulose-click-ferrocenes as docking spots for cyclodextrin. *Polymer International*, *61*(8), 1245–1248.
Senel, M., Cevik, E., & Abasiyanik, M. F. (2010). Amperometric hydrogen peroxide biosensor based on covalent immobilization of horseradish peroxidase on ferrocene containing polymeric mediator. *Sensors and Actuators B—Chemical*, *145*(1), 444–450.
Sirkar, K., & Pishko, M. V. (1998). Amperometric biosensors based on oxidoreductases immobilized in photopolymerized poly(ethylene glycol) redox polymer hydrogels. *Analytical Chemistry*, *70*(14), 2888–2894.
Tingaut, P., Hauert, R., & Zimmermann, T. (2011). Highly efficient and straightforward functionalization of cellulose films with thiol-ene click chemistry. *Journal of Materials Chemistry*, *21*(40), 16066–16076.
Tripathi, V. S., Kandimalla, V. B., & Ju, H. X. (2006). Amperometric biosensor for hydrogen peroxide based on ferrocene-bovine serum albumin and multiwall carbon nanotube modified ormosil composite. *Biosensors & Bioelectronics*, *21*(8), 1529–1535.
Trombino, S., Cassano, R., Bloise, E., Muzzalupo, R., Leta, S., Puoci, F., et al. (2008). Design and synthesis of cellulose derivatives with antioxidant activity. *Macromolecular Bioscience*, *8*(1), 86–95.
Villalonga, R., Diez, P., Yanez-Sedeno, P., & Pingarron, J. M. (2011). Wiring horseradish peroxidase on gold nanoparticles-based nanostructured polymeric network for the construction of mediatorless hydrogen peroxide biosensor. *Electrochimica Acta*, *56*(12), 4672–4677.
Wang, D. Q., Tan, J. J., Kang, H. L., Ma, L., Jin, X., Liu, R. G., et al. (2011). Synthesis, self-assembly and drug release behaviors of pH-responsive copolymers ethyl cellulose-*graft*-PDEAEMA through ATRP. *Carbohydrate Polymers*, *84*(1), 195–202.
Xu, F. J., Ping, Y., Ma, J., Tang, G. P., Yang, W. T., Li, J., et al. (2009). Comb-shaped copolymers composed of hydroxypropyl cellulose backbones and cationic poly((2-dimethyl amino)ethyl methacrylate) side chains for gene delivery. *Bioconjugate Chemistry*, *20*(8), 1449–1458.
Xu, S. X., Li, J. L., Zhou, Z. L., & Zhang, C. X. (2014). A third-generation hydrogen peroxide biosensor based on horseradish peroxidase immobilized by sol gel thin film on a multi-wall carbon nanotube modified electrode. *Analytical Methods*, *6*(16), 6310–6315.
Yang, W. W., Zhou, H., & Sun, C. Q. (2007). Synthesis of ferrocene-branched chitosain derivatives: Redox polysaccharides and their application to reagentless enzyme-based biosensors. *Macromolecular Rapid Communications*, *28*(3), 265–270.